The Transcriptional Activity of the APP Intracellular Domain−Fe65 Complex Is Inhibited by Activation of the NF-κB Pathway†

Quan Zhao and Frank S. Lee*

Department of Pathology and Laboratory Medicine, University of Pennsylvania School of Medicine, Philadelphia, Pennsylvania 19104

Received November 5, 2002; Revised Manuscript Received February 7, 2003

ABSTRACT: The β-amyloid precursor protein (APP) is an integral membrane protein that is the subject of proteolytic processing. Sequential cleavage of APP by β-secretase and subsequently γ-secretase generates the β-amyloid peptide as well as a cytoplasmic intracellular domain (AICD). AICD binds to the transcriptional coactivator Fe65, and this complex has been shown to display transcriptional activity. The regulation of this complex is poorly understood. We show here that activation of the NF-κB pathway, either by overexpression of NF-κB-inducing kinase (NIK) or by treatment with the proinflammatory cytokine IL-1β, downregulates the transcriptional activity of the AICD−Fe65 complex. This therefore provides a mechanism by which the activity of AICD might be modulated by extracellular stimuli. These results also identify an intracellular signal transduction pathway influenced by the NF-κB signaling pathway.

Substantial evidence implicates the β-amyloid precursor protein (APP)[1] in the pathogenesis of Alzheimer's disease (*1*). APP is an integral membrane protein that is initially synthesized as a series of alternatively spliced isoforms, ranging from 695 to 770 residues, which then undergo processing by a series of membrane-bound proteases that have been the subject of intense scrutiny (*2*). In one pathway, α-secretase (TNF-α converting enzyme) cleaves APP after Lys-612 (in the case of the A695 isoform) to yield an N-terminal ectodomain and a C-terminal membrane-bound fragment. In a second pathway, β-secretase cleaves APP after Met-596 to yield a distinct membrane-anchored C-terminal fragment (C99). The γ-secretases, which contain the presenilin-1 or presenilin-2 proteins as their catalytic subunits, then cleave the C99 fragment. Cleavage occurs within the transmembrane domain after either Val-636 or Ala-638, yielding Aβ40 (residues 597−636) or Aβ42 (residues 597−638), respectively. In addition, this generates a C-terminal fragment that is subsequently cleaved after Leu-645, yielding an APP intracellular domain (AICD, consisting of residues 646−695) (*3*). The Aβ peptide is the central component of extracellular amyloid plaques, a histologic hallmark of Alzheimer's disease. The Aβ42 peptide, as opposed to the Aβ40 peptide, is thought to be particularly pathogenic, with both the absolute quantity and ratio of Aβ42:Aβ40 playing critical roles in the pathogenesis of the amyloid plaques (*1*−*3*).

Substantially less is known regarding the fate of the AICD. Several groups have employed yeast two-hybrid screens to demonstrate an interaction between AICD and the family of Fe65 transcriptional coactivators (*4*−*6*). Fe65 binds to a NPTY sequence motif in AICD (*6*−*8*). Furthermore, it has been shown that the AICD−Fe65 complex displays transcriptional activity in reporter gene assays employing GAL4 fusion proteins (*9*, *10*). Hence, AICD may behave as a transcription factor, analogous to the behavior of the Notch intracellular domain (NICD), which is generated by the sequential cleavage of Notch by the same α- and γ-secretases that process APP (*11*). NICD binds to the CSL family of transcription factors and influences many different cellular processes, including proliferation, differentiation, and apoptosis (*12*−*14*).

The activities of many transcription factors can be regulated by extracellular stimuli and are the targets of intracellular signaling pathways. Two broad classes of stimuli include growth factors and stress. A central pathway activated by the former is the extracellular-regulated protein kinase (ERK) pathway (*15*), while two important pathways activated by the latter are the c-Jun N-terminal kinase (JNK; also known as stress-activated protein kinase) and NF-κB pathways (*16*, *17*). All three of these pathways consist of protein kinase cascades, and the family of mitogen-activated protein kinase kinase kinases (MAP3Ks) plays central roles in all three of them (*18*). In the ERK pathway, the MAP3K Raf phosphorylates and activates the mitogen-activated protein kinase kinase (MAP2K) MEK, which in turn phosphorylates and activates ERK. An important substrate of ERK is the transcription factor Elk-1, a component of the ternary complex that assembles at the serum response element of genes that are typically involved in immediate early responses to serum stimulation.

The JNK and NF-κB pathways can be activated by a wide variety of stresses, including proinflammatory cytokines such as IL-1β and TNF-α, lipopolysaccharide, virus infection, and oxidative stress (*16*, *17*, *19*). In the JNK pathway, MAP3Ks

† This work was supported by a Beeson Scholarship to F.S.L. from the American Federation for Aging Research.

* Address correspondence to this author at the Department of Pathology and Laboratory Medicine, University of Pennsylvania School of Medicine, 605 Stellar Chance Labs, 422 Curie Blvd., Philadelphia, PA 19104. Tel: 215-898-4701. Fax: 215-573-2272. E-mail: franklee@mail.med.upenn.edu.

[1] Abbreviations: Aβ, β-amyloid; AICD, APP intracellular domain; APP, β-amyloid precursor protein; IKK, IκB kinase; GAL4, DNA binding domain of the GAL4 protein; JNK, c-Jun N-terminal kinase; MAPK, mitogen-activated protein kinase; MAP2K, mitogen-activated protein kinase kinase; MAP3K, mitogen-activated protein kinase kinase kinase; NIK, NF-κB-inducing kinase.

10.1021/bi027117f CCC: $25.00
Published on Web 03/08/2003

that include ASK1, MEKK1, and MLK3 phosphorylate and activate MAP2Ks that include MKK4 and MMK7, which then phosphorylate and activate JNK (*16*). JNK then phosphorylates and activates transcription factors that include c-Jun and ATF2. c-Jun in combination with c-fos forms the AP1 transcription factor complex. c-Jun and ATF2, as well as NF-κB, influence the activation of many genes, particularly those involved in immune and inflammatory responses.

In the NF-κB pathway, MAP3Ks phosphorylate and activate the IκB kinases (IKKs), which consist of two isoforms, IKKα and IKKβ. IKK phosphorylates IκB, the NF-κB inhibitor, which under resting conditions sequesters NF-κB in the cytoplasm (*17*, *19*). This phosphorylation targets IκB for degradation, allowing the nuclear translocation of NF-κB. In response to stimuli such as IL-1β or TNF-α, IKKβ phosphorylates IκB and thereby targets it for degradation. In a parallel pathway activated in response to stimuli such as lymphotoxin-β, IKKα phosphorylates the p100 NF-κB subunit, promoting its processing to the p52 subunit of the transcription factor NF-κB (*20*). Notably, in response to certain stimuli, such as RANKL/TRANCE, IKKα also phosphorylates IκB, thereby providing a second mechanism by which IKKα can activate NF-κB (*21*). The specific MAP3Ks involved in NF-κB signaling are an area of active investigation. Current evidence indicates that the MAP3K NF-κB-inducing kinase (NIK) is an IKKα activator (*20*, *22*, *23*), while the MAP3K MEKK3 has been implicated in TNF-α-induced IKK activation (*24*).

To test whether the activity of the AICD−Fe65 complex might be regulated by these pathways, we examined the effects of activation of these pathways on the transcriptional activity of the AICD−Fe65 complex. We report here that activation of the NF-κB pathway results in inhibition of the transcriptional activity of the AICD−Fe65 complex. The data therefore indicate that the activity of the AICD−Fe65 complex can in principle be modulated and, conversely, potentially point to a novel role for the NF-κB signaling pathway in Alzheimer's disease.

EXPERIMENTAL PROCEDURES

Plasmids. pBXG-APP (652−695) was constructed by PCR amplification of the indicated coding sequence of APP from pcDNA3.1-APP (a gift of Dr. Virginia Lee, University of Pennsylvania School of Medicine) using the BGH reverse primer and the following primer: 5′-CGGAATTCCAGTACACATCCATTCATCATGG-3′. The resulting product was digested with *Eco*RI/*Xba*I and subcloned into the *Eco*RI/*Xba*I site of pBXG1. pcDNA3-GAL4-APP (652−695) was constructed by subcloning the 0.6 kb *Hin*dIII fragment of pBXG-APP (652−695) into the *Hin*dIII site of pcDNA3. The P685A/Y687A mutant of APP (652−695) was constructed using a QuikChange mutagenesis kit (Stratagene).

pcDNA3-FlagFe65 was constructed by subcloning the 2.2 kb *Sma*I (partial)/*Xba*I fragment of Gene Connection Discovery Clone C47586 (Stratagene), which contains the complete human Fe65 coding sequence, into the *Xho*I (blunt)/*Xba*I site of pcDNA3-Flag, a vector derived from pcDNA3 containing the coding sequence for the Flag epitope. pENTR-FlagFe65 was constructed by subcloning the 2.2 kb *Kpn*I/*Xba*I fragment of pcDNA3-FlagFe65 into the *Kpn*I/*Xba*I site of pENTR3 (Invitrogen). pBXG-cJun (1−79) was constructed by first subcloning the 0.24 kb *Bam*HI/*Not*I fragment of pGEX-cJun (1−79) into the *Bam*HI/*Not*I site of pBS SK and then subcloning the 0.25 kb *Eco*RI fragment of the resulting product into the *Eco*RI site of pBXG1. pcDNA3-GAL-AD was constructed by subcloning the 0.5 kb *Kpn*I (blunt)/*Bam*HI fragment of pGADT7 (BD Biosciences Clontech) into the *Eco*RI (blunt)/*Bam*HI site of pcDNA3-GAL4, a vector derived from pcDNA3 containing the coding sequence for the DNA binding domain of GAL4.

pRK-mycNIK and pRK-mycNIK (K429A/K430A) were gifts of Dr. Warner Greene (Gladstone Institute of Virology and Immunology, San Francisco, CA). pcDNA3-Raf BXB was a gift of Dr. Carlos Paya (Mayo Clinic, Rochester, MN). The G5E1b-Luc reporter gene and pGAL4-ATF2 (1-109) were gifts of Dr. Roger Davis (University of Massachusetts Medical Center, Worcester, MA). MLV-GAL4-Elk C was a gift of Dr. Richard Treisman (Imperial Cancer Research Fund, London, U.K.). pC6-Tip60α and pC6-Tip60β were gifts of Dr. Olivia M. Pereira-Smith (Baylor College of Medicine, Houston, TX). The sources of pcDNA3-ASK1, pCMV4-FlagIκBα (S32A/S36A), NF-κB-Luc, and AP1-Luc have been described (*25*, *26*).

Where appropriate, sequences of recombinant plasmids were confirmed using a Big Dye Terminator kit and an ABI automated sequencer.

Cell Culture and Transfections. HeLa, COS-7, and N2a cells were maintained in DMEM supplemented with 10% fetal bovine serum, 100 IU/mL penicillin, and 100 μg/mL streptomycin. Transient transfections were performed using Fugene 6 (Roche) according to the manufacturer's instructions. Cells were split into 24-well (for luciferase assays) or 6-well (for coimmunoprecipitation assays) plates so as to achieve 60−70% confluency and then transfected using a 2:1 Fugene:DNA ratio. Cells were typically harvested 42 h posttransfection. Human TNF-α and mouse interleukin-1β were obtained from Roche.

Luciferase Assays. Cells were washed once with PBS, harvested in Passive lysis buffer (Promega), and centrifuged at 15000*g* for 10 min at 4 °C. Aliquots of the cleared lysates were then assayed using a dual luciferase reporter assay system (Promega) and a Wallac LB9507 luminometer.

Recombinant Proteins. pDEST10-FlagFe65 was prepared through a GATEWAY clonase reaction between pENTR-FlagFe65 and pDEST10 (Invitrogen). Preparation of recombinant baculovirus and purification of recombinant $(His)_6$Flag-Fe65 using Ni-NTA−agarose were performed according to the manufacturer's instructions. ^{35}S-Labeled, in vitro translated $(His)_6$myc-Tip60α was prepared using a TnT kit (Promega) and pC6-Tip60α as the template.

Immunoprecipitations and Western Blotting. Cells were washed once with Dulbecco's PBS containing 1 mM EDTA and then lysed by the addition of 1 mL of buffer L (20 mM Tris, pH 7.6, 150 mM NaCl, 25 mM β-glycerophosphate, 2 mM EDTA, 2 mM pyrophosphate, 10% glycerol, 1% Triton X-100, 1 mM DTT, 1 mM orthovanadate) containing 10 μg/mL leupeptin and 1 mM phenylmethanesulfonyl fluoride. Supernatants were obtained after centrifugation of the whole cell lysate at 16000*g* for 10 min at 4 °C. Protein concentrations of the supernatant were measured with the Bradford reagent (Bio-Rad).

In one series of experiments, the supernatant was incubated with 10 μL of M2−agarose with rocking for 1 h at 4 °C.

The resin was washed three times with buffer L and then incubated with 5 μL of ^{35}S-labeled, in vitro translated $(His)_6$myc-Tip60α in 500 μL of buffer A (20 mM Hepes, pH 7.6, 0.1 M KCl, 10% glycerol, 0.2% NP-40, 1 mM DTT) containing 0.2% BSA for an additional 1 h at 4 °C with rocking. The resin was then washed three times with buffer A and eluted by the addition of 20 μL of 2× SDS−PAGE loading buffer. In a second series of experiments, the supernatant was incubated with 1 μg of $(His)_6$Flag-Fe65 with rocking at 4 °C for 1 h. The latter was then immunoprecipitated by incubation with 10 μL of M2−agarose with rocking for 1 h at 4 °C. The resin was then washed three times with buffer L and eluted by the addition of 20 μL of 2× SDS−PAGE loading buffer.

Immunoprecipitates or aliquots of cell lysates were subjected to SDS−PAGE and, in some cases, were then transferred to Immobilon-P membranes (Millipore). The membranes were blotted with anti-GAL4 (RK5C1, Santa Cruz Biotechnology), anti-Myc (9E10, University of Pennsylvania Cell Center), or anti-Flag (M2, Sigma) monoclonal antibodies or anti-Myc (A-14, Santa Cruz Biotechnology) polyclonal antibodies. Western blots were performed as described (*25*).

RESULTS

Previous work has shown that transcriptional activity of a GAL4-APP (652−695) fusion protein is augmented by Fe65, thereby providing evidence that they form a transcriptionally active complex (*9*). In similar experiments, we transfected Hela, COS-7, or N2a cells with a luciferase reporter gene driven by GAL4 binding sites and expression constructs for the DNA binding domain of GAL4 (hereafter referred to as GAL4) or GAL4-APP (652−695) in the absence or presence of one for Fe65. Forty-two hours posttransfection, luciferase activity was then measured. As shown in Figure 1, and in agreement with the previous report, we find that GAL4-APP (652-695) has modest transcriptional activity and that this activity can be substantially enhanced by coexpression with Fe65 in Hela, COS-7, and N2a cells. The activity of GAL4 fused to a longer fragment of APP (637−695) was also enhanced by coexpression with Fe65 (data not shown). In addition, and in agreement with published data (*9*), we found that the enhancement is abolished by the P685A/Y687A mutant of APP (652−695) and that ^{35}S-labeled, in vitro translated Fe65 was able to bind GST-APP (652−695) in vitro (data not shown).

Many transcription factor complexes are responsive to extracellular stimuli. We therefore considered whether the AICD−Fe65 complex might be responsive to pathways regulated by extracellular stimuli. In initial experiments, we examined whether overexpression of MAP3Ks that activate these various pathways can influence the transcriptional activity of the AICD−Fe65 complex. Toward this end, Hela cells were cotransfected with the GAL4 reporter gene, expression constructs for GAL4-APP (652−695) and Fe65, and constructs for c-Raf, ASK1, or NIK. These three MAP3Ks have the capacity to activate the ERK, JNK, and NF-κB pathways, respectively. As shown in Figure 2A, the GAL4-APP (652−695)−Fe65 complex has transcriptional activity substantially higher than that of GAL4, as expected. This activity is not substantially influenced by ASK1 and is

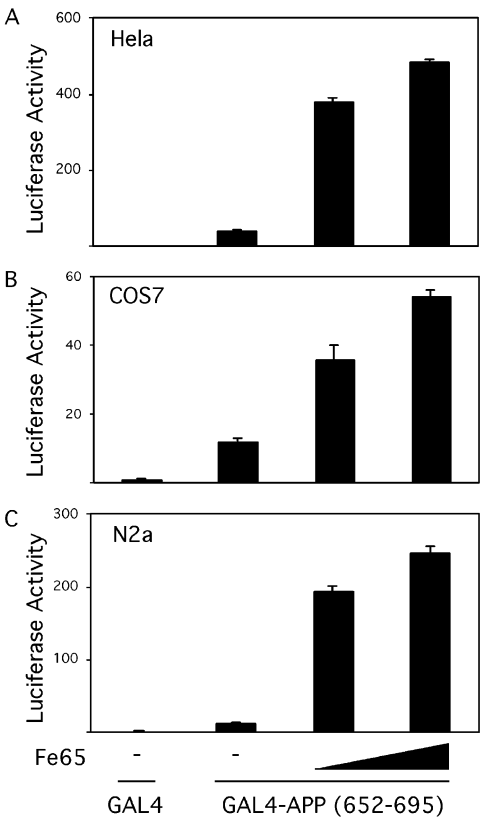

FIGURE 1: Fe65 potentiation of AICD transcriptional activity. (A) Hela, (B) COS-7, or (C) N2a cells were cotransfected with 0.1 μg of G5E1b-Luc, 0.05 μg of pRL-TK, and 0.1 μg of pcDNA3-GAL4 or 0.1 μg of pcDNA3-GAL4-APP (652−695) with or without 0.1 or 0.2 μg of pcDNA3-FlagFe65. The total DNA dose was adjusted to 0.45 μg with pcDNA3. Cells were harvested, and luciferase activities were measured and normalized to that of Renilla luciferase. Shown is a representative result, performed in duplicate, of three independent experiments.

only modestly stimulated by c-Raf. In contrast, coexpression with NIK results in marked inhibition of activity. Control experiments demonstrate the capacity of c-Raf to activate a GAL4-Elk (307−428) fusion protein, ASK1 to activate an AP1 reporter gene, and NIK to activate an NF-κB reporter gene (Figure 2B).

We compared the effect of NIK toward AICD−Fe65 with its effect on the transcriptional activation domains of three other transcription factors, ATF2 (residues 1−109), c-Jun (residues 1−79), and GAL4 (residues 768−881, hereafter referred to as AD). As shown in Figure 3A,B, under conditions where NIK markedly inhibits the transcriptional activity of the GAL4-APP (652−695)−Fe65 complex, it has at best only modest effects on GAL4-ATF2 (1−109), GAL4-cJun (1−79), or GAL4-AD. Thus, NIK displays a degree of inhibitory activity toward the AICD−Fe65 complex that is not particularly seen with these other transcription factors. In addition, the inhibition of AICD−Fe65 activity by NIK was seen not only in Hela and COS-7 cells but also in N2a cells (Figure 3C).

To examine whether the inhibitory activity of NIK toward AICD−Fe65 depends on the catalytic activity of the former, Hela cells were cotransfected with the GAL4 reporter gene, constructs for GAL4-APP (652−695) and Fe65, and constructs for either wild-type NIK or a mutant NIK (K429A/K430A). The latter is defective in ATP binding and therefore

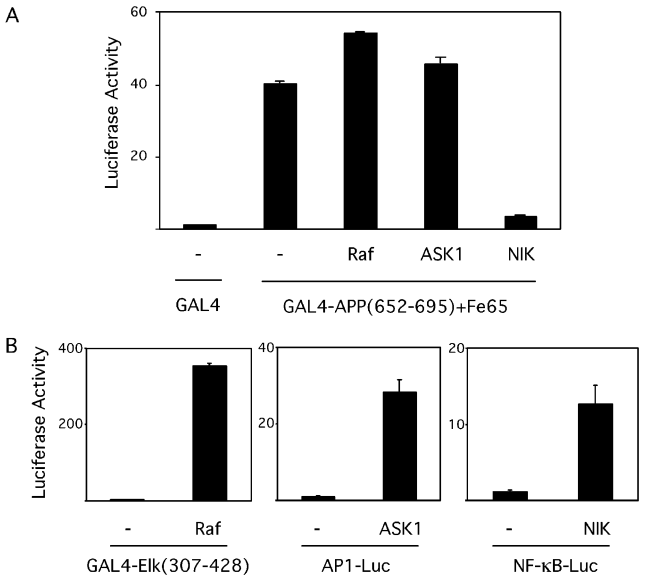

FIGURE 2: NIK-induced inhibition of AICD−Fe65 activity. (A) Hela cells were cotransfected with 0.1 μg of G5E1b-Luc, 0.05 μg of pRL-TK, and 0.2 μg of pcDNA3-GAL4 or the combination of 0.1 μg of pcDNA3-GAL4-APP (652−695) and 0.1 μg of pcDNA3-FlagFe65 in the absence or presence of 0.1 μg of pcDNA3, pcDNA3-Raf BXB, pcDNA3-ASK1, or pRK-mycNIK. (B) Hela cells were cotransfected with 0.05 μg of MLV-GAL4-Elk C, 0.05 μg of G5E1b-Luc, 0.05 μg of pRL-TK, and 0.1 μg of either pcDNA3 or pcDNA3-Raf BXB (left); 0.1 μg of AP1-Luc, 0.05 μg of pRL-TK, and 0.1 μg of either pcDNA3 or pcDNA3-ASK1 (middle); or 0.1 μg of NF-κB-Luc, 0.05 μg of pRL-TK, and 0.1 μg of either pcDNA3 or pRK-mycNIK (right). Cells were harvested, and luciferase activities were measured and normalized to that of Renilla luciferase. Shown is a representative result, performed in duplicate, of two independent experiments.

catalytically inactive (*22*, *27*). As shown in Figure 4A, under conditions where coexpression with wild-type NIK inhibits the activity of AICD−Fe65 complex, catalytically inactive NIK does not; indeed, a slight elevation of reporter gene is observed. Thus, NIK-induced inhibition of the AICD−Fe65 complex depends on the protein kinase activity of NIK.

In transient transfection assays, NIK is a potent inducer of activity from NF-κB-dependent reporter genes. We therefore next compared the ability of NIK to inhibit the transcriptional activity of the AICD−Fe65 complex to its ability to activate an NF-κB reporter gene. Hela cells were cotransfected with varying doses of NIK expression vector and either a luciferase reporter gene driven by NF-κB binding sites or the GAL4 reporter gene in combination with the GAL4-APP (652−695) and Fe65 expression vectors. As shown in Figure 4B, NIK both inhibits the activity of the AICD−Fe65 complex and activates the NF-κB reporter gene in a dose-dependent manner. Significantly, there is no evidence of saturation of either transcriptional response, suggesting that the inhibition of the AICD−Fe65 complex is not simply occurring under conditions in which the NF-κB-induced response has been saturated.

In the NF-κB pathway, NIK can activate IKKα, thereby promoting the processing of p100 to the p52 subunit of NF-κB (*17*). IKKα also has the capacity to phosphorylate IκB and target it for degradation, thereby liberating NF-κB to translocate to the nucleus (*21*). In the case of IκBα, the most extensively studied isoform, phosphorylation occurs on Ser-32 and Ser-36 (*28*, *29*). A mutant IκBα in which the

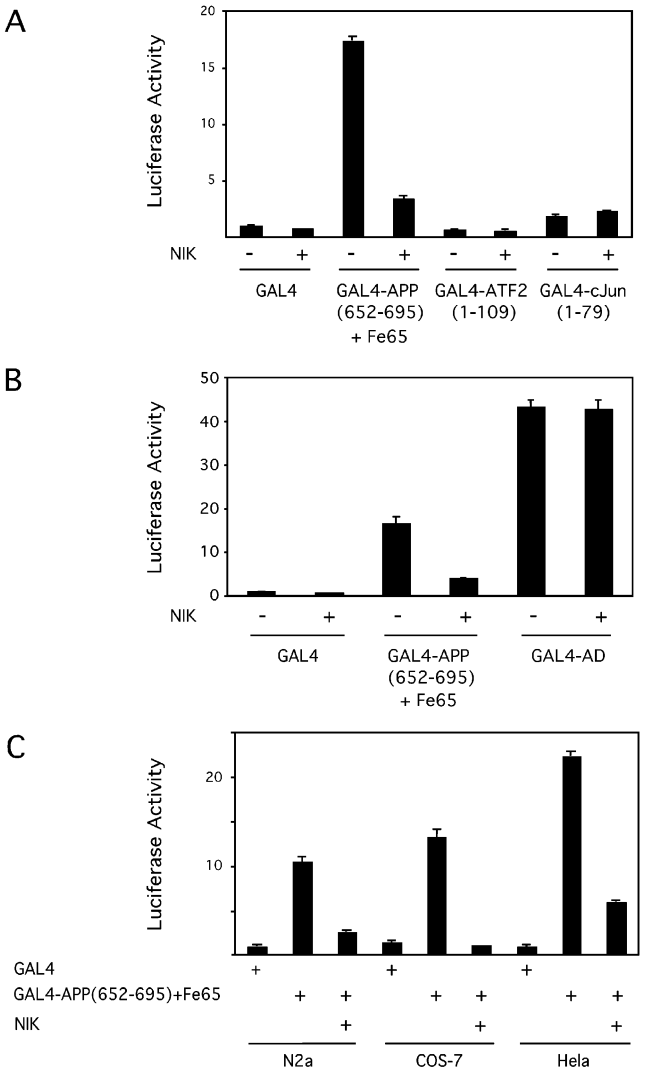

FIGURE 3: Specificity of NIK-induced inhibition of AICD−Fe65. (A) Hela cells were cotransfected with 0.1 μg of G5E1b-Luc, 0.05 μg of pRL-TK, and either 0.2 μg of pcDNA3-GAL4, a combination of 0.1 μg of pcDNA3-GAL4-APP (652−695) and 0.1 μg of pcDNA3-FlagFe65, 0.2 μg of pGAL4-ATF2 (1−109), or 0.2 μg of pBXG-cJun (1−79) in the absence or presence of 0.1 μg of pRK-mycNIK. The total DNA dose was adjusted to 0.45 μg with pcDNA3. Cells were harvested, and luciferase activities were measured and normalized to that of Renilla luciferase. Shown is a representative result, performed in duplicate, of three independent experiments. (B) COS-7 cells were cotransfected with 0.1 μg of G5E1b-Luc, 0.05 μg of pRL-TK, and either 0.1 μg of pcDNA3-GAL4, a combination of 0.1 μg of pcDNA3-GAL4-APP (652−695) and 0.1 μg of pcDNA3-FlagFe65, or 1 ng of pcDNA3-GAL4-AD in the absence or presence of 0.05 μg of pRK-mycNIK. The total DNA dose was adjusted to 0.4 μg with pcDNA3. Cells were harvested, and luciferase activities were measured and normalized to that of Renilla luciferase. Shown is a representative result, performed in duplicate, of two independent experiments. (C) N2a, COS-7, or Hela cells were cotransfected with 0.1 μg of G5E1b-Luc, 0.05 μg of pRL-TK, and either 0.2 μg pcDNA3-GAL4 or a combination of 0.1 μg of pcDNA3-GAL4-APP (652−695) and 0.1 μg of pcDNA3-FlagFe65 in the absence or presence of 0.2 μg of pRK-mycNIK. The total DNA dose was adjusted to 0.55 μg with pcDNA3. Cells were harvested, and luciferase activities were measured and normalized to that of Renilla luciferase. Shown is a representative result, performed in duplicate, of three independent experiments.

phosphoacceptor residues at these positions have been mutated to alanine (S32A/S36A) is refractory to degradation and serves as a potent dominant negative inhibitor of NF-

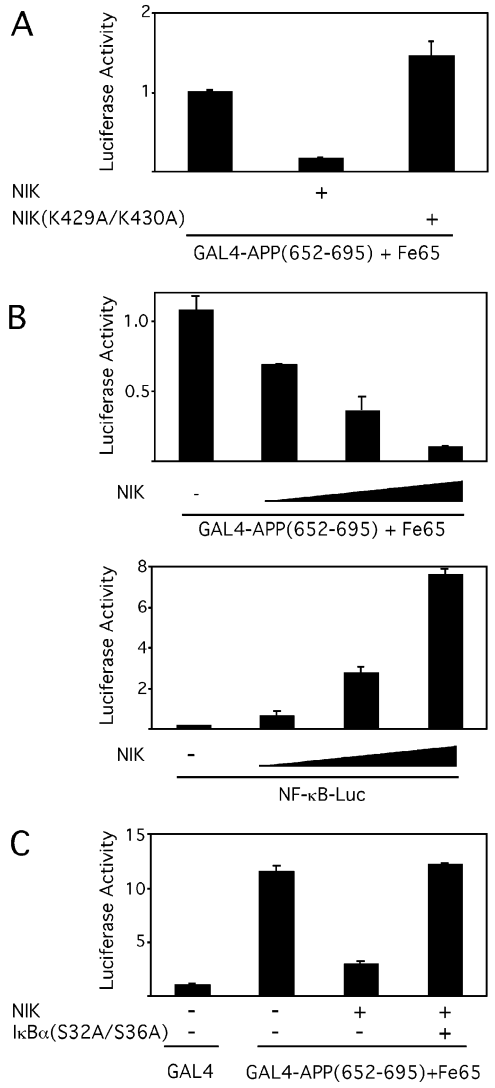

FIGURE 4: Dependence on catalytic activity of NIK-induced inhibition of AICD−Fe65. (A) Hela cells were cotransfected with 0.1 μg of G5E1b-Luc, 0.05 μg of pRL-TK, 0.1 μg of pcDNA3-GAL4-APP (652−695), 0.1 μg of pcDNA3-FlagFe65, and 0.2 μg of either pcDNA3, pRK-mycNIK, or pRK-mycNIK (K429A/K430A). Cells were harvested, and luciferase activities were measured and normalized to that of Renilla luciferase. Shown is a representative result, performed in duplicate, of two independent experiments. (B) Titration of NIK-induced inhibition of AICD−Fe65 (top) and activation of NF-κB (bottom). Hela cells were cotransfected with 0.002, 0.02, or 0.2 μg of pRK-mycNIK and either (top) 0.1 μg of pcDNA3-GAL4-APP (652−695), 0.1 μg of pcDNA3-FlagFe65, 0.1 μg of G5E1b-Luc, and 0.05 μg of pRL-TK or (bottom) 0.15 μg of NF-κB-Luc and 0.05 μg of pRL-TK. The total DNA dose was adjusted to (top) 0.55 μg or (bottom) 0.4 μg with pcDNA3. Cells were harvested, and luciferase activities were measured and normalized to that of Renilla luciferase. Shown is a representative result, performed in duplicate, of two independent experiments. (C) Reversal of NIK-induced inhibition of AICD−Fe65. Hela cells were cotransfected with 0.1 μg of G5E1b-Luc, 0.05 μg of pRL-TK, and 0.2 μg of pcDNA3-GAL4 or the combination of 0.1 μg of pcDNA3-GAL4-APP (652−695) and 0.1 μg of pcDNA3-FlagFe65 in the absence or presence of 0.1 μg of pRK-mycNIK with or without 0.1 μg of pCMV4-FlagIκBα (S32A/S36A). The total DNA dose was adjusted to 0.55 μg with pcDNA3. Cells were harvested, and luciferase activities were measured and normalized to that of Renilla luciferase. Shown is a representative result, performed in duplicate, of two independent experiments.

κB activity (*28*, *29*). To provide further evidence that NIK inhibition is occurring through activation of the NF-κB pathway, we cotransfected Hela cells with the GAL4 reporter gene and constructs for NIK in the absence or presence of a construct for IκBα (S32A/S36A). As shown in Figure 4C, NIK inhibits the transcriptional activity of the AICD−Fe65 complex, consistent with previous results. Significantly, this inhibition is abolished by coexpression with the dominant negative IκBα, providing additional evidence that NIK inhibition of the AICD−Fe65 complex is mediated through NF-κB.

The NF-κB pathway can be activated by a broad range of stimuli, including the proinflammatory cytokines TNF-α or IL-1β, lipopolysaccharide, and virus infection, among others (*30*). In Figure 5A, we examined whether TNF-α or IL-1β might be able to influence the activity of the AICD−Fe65 complex. Thus, COS-7 cells were cotransfected with the GAL4 reporter gene and constructs for GAL4-APP (652−695) and Fe65. Some cells were then stimulated with TNF-α or IL-1β, and luciferase activities then measured. As with NIK overexpression, treatment of cells with either TNF-α or IL-1β inhibited the transcriptional activity of the AICD−Fe65 complex (by 60% and 44%, respectively). Western blotting of lysates reveals that, if anything, these proinflammatory cytokines augment the level of the GAL4-APP (652−695) and Fe65 proteins. Hence, these cytokines inhibit the transcriptional activity of the APP (652−695)−Fe65 complex.

Fe65 binds to the transcriptional coactivator Tip60, thereby providing a possible explanation for the transcriptional activity of the AICD−Fe65 complex (*9*, *31*). One potential mechanism by which IL-1β might inhibit the transcriptional activity of the AICD−Fe65 complex is by weakening the Fe65−Tip60 interaction. To examine this, we transfected COS-7 cells with an expression vector for FlagFe65, stimulated some cells with IL-1β, and then prepared cellular lysates. The Fe65 was immunoprecipitated with anti-Flag antibodies and then examined for its capacity to bind ^{35}S-labeled, in vitro translated $(His)_6$myc-Tip60. As shown in Figure 5B, Fe65 interacts with Tip60 (compare lanes 2 and 3, top panel), as expected. This interaction, however, is unchanged by IL-1β stimulation (compare lanes 3 and 4, top panel). In a converse approach, we transfected COS-7 cells with an expression vector for Tip60, stimulated some cells with IL-1β, and then prepared cellular lysates. These lysates were incubated with recombinant FlagFe65, and the latter was immunoprecipated with anti-Flag antibodies. The immunoprecipitates were then examined for the absence or presence of Tip60. As shown in Figure 5C, Tip60 interacts with Fe65 (compare lanes 2 and 3, top panel), as expected, but this interaction is unchanged by IL-1β stimulation (lane 4, top panel). Collectively, these results indicate that, under the experimental conditions employed, IL-1β does not affect the Fe65−Tip60 interaction.

IL-1β can activate not only the NF-κB pathway but also other intracellular signaling pathways (*32*). To examine if the IL-1β-induced inhibition of AICD−Fe65 activity is specifically mediated through the NF-κB pathway, we performed an experiment similar to that shown in Figure 5A but, in this case, in the presence of the dominant negative IκBα. As shown in Figure 6, under conditions where dominant negative IκBα inhibits IL-1β-induced activation of an NF-κB reporter gene (Figure 6B), it also relieves the IL-1β-induced inhibition of the AICD−Fe65 complex (Fig-

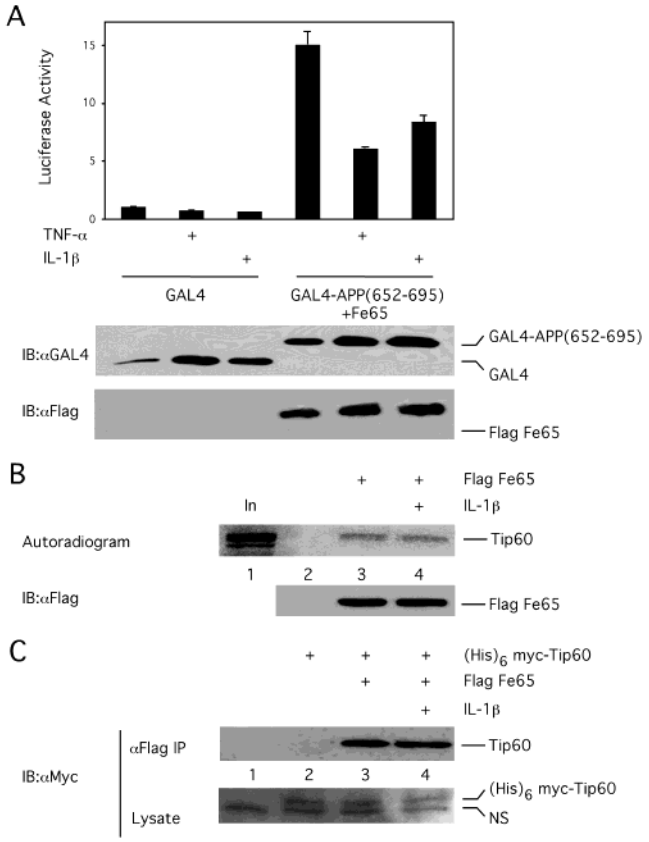

FIGURE 5: Cytokine-induced inhibition of AICD−Fe65. (A) COS-7 cells were cotransfected with 0.1 μg of G5E1b-Luc, 0.05 μg of pRL-TK, and 0.1 μg of pcDNA3-GAL4 or the combination of 0.1 μg of pcDNA3-GAL4-APP (652−695) and 0.1 μg of pcDNA3-FlagFe65. The total DNA dose was adjusted to 0.35 μg with pcDNA3. Twenty-four hours posttransfection, some cells were treated with either 20 ng/mL TNF-α or 10 ng/mL IL-1β for 18 h. Cells were harvested, and luciferase activities were measured and normalized to that of Renilla luciferase. Aliquots of cell lysates were also subjected to immunoblotting with anti-GAL4 (top panel) or anti-Flag (bottom panel) monoclonal antibodies. The positions of GAL4, GAL4-APP (652−695), and FlagFe65 are indicated to the right. Shown is a representative result, performed in duplicate, of three independent experiments. (B) COS-7 cells were mock treated (lane 2) or transfected (lanes 3 and 4) with 1 μg of pcDNA3-FlagFe65, and 18 h later, some cells treated with 10 ng/mL IL-1β for 30 min. Cellular lysates were subjected to immunoprecipitation with anti-Flag antibodies and then incubated with ^{35}S-labeled, in vitro translated (His)$_6$myc-Tip60α. Bound (His)$_6$myc-Tip60α was subjected to SDS−PAGE and autoradiography (top panel). Aliquots of the cell lysates were examined by immunoblotting with anti-Flag antibodies (bottom panel). In denotes 10% of input (His)$_6$myc-Tip60α. One of three representative results is shown. (C) COS-7 cells were transfected with 1 μg of pC6-Tip60β as indicated, and 22 h later, some cells treated with 10 ng/mL IL-1β for 30 min. Cell lysates (900 μg) were then incubated with recombinant (His)$_6$Flag-Fe65 and then subjected to immunoprecipitation with anti-Flag antibodies. The immunoprecipitates (top panel) or aliquots of the cell lysates (bottom panel) were examined by immunoblotting with anti-Myc polyclonal or monoclonal antibodies, respectively. NS denotes nonspecific band. One of two representative results is shown.

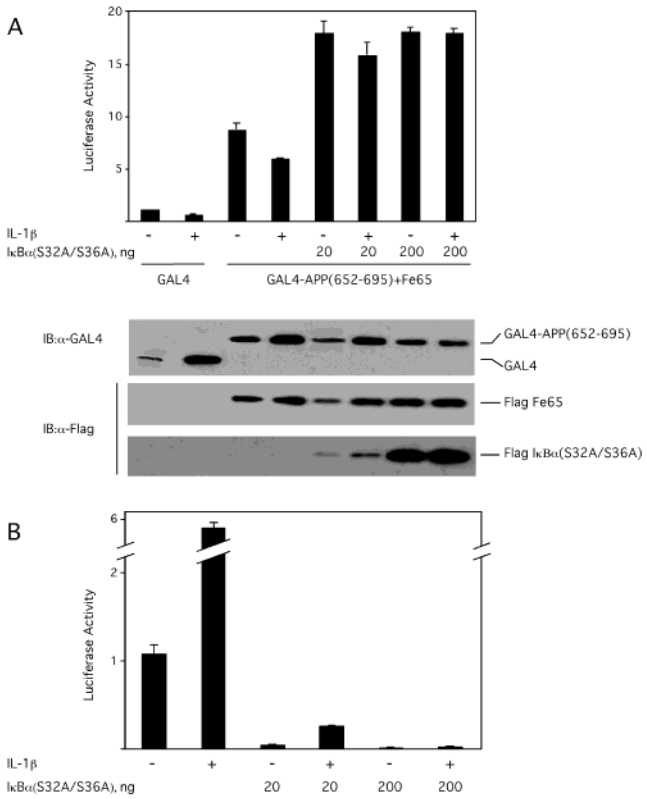

FIGURE 6: Reversal of IL-1β-induced inhibition of AICD−Fe65. COS-7 cells were cotransfected with either 0, 20, or 200 ng of pCMV4-FlagIκBα (S32A/S36A) as indicated and either (A) 0.1 μg of G5E1b-Luc, 0.05 μg of pRL-TK, and 0.2 μg of pcDNA3-GAL4 or the combination of 0.1 μg of pcDNA3-GAL4-APP (652−695) and 0.1 μg of pcDNA3-FlagFe65 or (B) 0.1 μg of NF-κB-Luc and 0.05 μg of pRL-TK. The total DNA dose was adjusted to (A) 0.55 μg or (B) 0.35 μg with pcDNA3. Twenty-four hours posttransfection, some cells were treated with 10 ng/mL IL-1β for 18 h. Cells were harvested, and luciferase activities were measured and normalized to that of Renilla luciferase. Aliquots of cell lysates were also subjected to immunoblotting (B) with anti-GAL4 (top panel) or anti-Flag (bottom two panels) antibodies. The positions of GAL4, GAL4-APP (652−695), FlagFe65, and FlagIκBα (S32A/S36A) are indicated to the right. Shown is a representative result, performed in duplicate, of two independent experiments.

ure 6A) in a dose-dependent manner. Thus, at doses of 0, 20, and 200 ng of IκBα (S32A/S36A) expression vector, the degree of IL-1β-induced inhibition [taking into account the stimulatory effect of IκBα (S32A/S36A) on the baseline activity of AICD−Fe65] was 32%, 12%, and 1%, respectively. We conclude that IL-1β inhibition of the transcriptional activity of the AICD−Fe65 complex is indeed mediated by the NF-κB pathway.

DISCUSSION

The past decade has witnessed dramatic progress in our understanding of the molecular mechanisms by which APP is processed to yield the pathogenic Aβ peptides of Alzheimer's disease (*2*). Up until relatively recently, the fate of the AICD liberated by this process has been less certain. Reports now indicate that AICD possesses transcriptional activity (*9*, *10*, *31*, *33*, *34*). Thus, there is a notable parallel in the processing of both APP and Notch by γ-secretase, each of which yields cytoplasmic fragments that possess transcriptional activity (*2*). A central question is whether this activity is constitutive or whether it can be regulated or influenced by other factors.

In this report, we provide evidence that the NF-κB pathway inhibits the transcriptional activity of the AICD−Fe65 complex. Specifically, we show that activation of the NF-κB pathway by NIK or the proinflammatory cytokine IL-1β inhibits the transcriptional activity of the AICD−Fe65

complex. The NIK-induced inhibition occurs with a dose−response curve that parallels that of its activation of an NF-κB reporter gene. Furthermore, inhibition induced by NIK or IL-1β can be relieved by overexpression of dominant negative IκBα, a potent dominant negative inhibitor of the NF-κB pathway, providing evidence that this inhibition is mediated through the NF-κB pathway.

The identification of the NF-κB pathway as a modulatory pathway for AICD is of significance from a number of perspectives. First, there is increasing evidence that immune and inflammatory reactions play central roles in the pathogenesis of Alzheimer's disease (*35*), and NF-κB is one of the central transcription factors activated in these settings. Indeed, the proinflammatory cytokines IL-1β and TNF-α are potent activators of the NF-κB pathway, and they have been directly implicated in Alzheimer's disease (*36*, *37*). It is likely that activated microglia and astrocytes in the vicinity of β-amyloid plaques are the source of these cytokines. Thus, cells in the vicinity of β-amyloid plaques are in a physiologic environment conducive to NF-κB activation, consistent with immunohistochemical studies that demonstrate increased levels of NF-κB protein in the cerebral cortical sections from Alzheimer's disease patients (*38*, *39*). It therefore follows that AICD activity in these cells may be influenced by cytokine-induced NF-κB activation. There is also evidence that Aβ itself can activate NF-κB in neurons (*39*, *40*), thereby providing an independent mechanism for NF-κB activation.

Second, there is evidence, albeit controversial, that apoptosis plays a role in the neurodegeneration of Alzheimer's disease (*41*), and an important activity of NF-κB is antiapoptosis (*42*). Thus, activation of the NF-κB pathway may serve to blunt proapoptotic influences, such as exposure to the Aβ peptide, that might serve to promote neurodegeneration. Conversely, its inhibition might accentuate Aβ-induced apoptosis (*43*). NF-κB antiapoptosis occurs, in part, through the induction of genes that include cIAP1, cIAP2, TRAF1, TRAF2, Bcl-2, and Bcl-x (*44*−*47*). It might also be noted that overexpression of AICD itself, as opposed to Aβ, in the neuroglioma cell line H4 can induce apoptosis (*48*). In this regard, the present studies would provide another mechanism by which the NF-κB pathway might exert its antiapoptic effects: through the inhibition of the transcriptional activity of AICD. Interestingly, the AICD-induced apoptosis occurs in an Fe65-independent manner (*48*).

Third, the secretases that generate Aβ are targets for pharmaceutical intervention, and their inhibition would be predicted to have effects on AICD generation (*2*). Thus, for example, just as this inhibition of γ-secretase might inhibit Notch signaling, this inhibition might also block AICD generation. By inhibiting AICD generation, this would be predicted to diminish AICD-dependent transcriptional activity, with a final result that might be similar to the inhibition induced by NF-κB activation. Conversely, inhibition of the NF-κB pathway might be predicted to relieve inhibitory effects on AICD and perhaps even increase the basal level of AICD activity (Figure 6). It is relevant to note the current interest in employing antiinflammatory agents in the treatment of Alzheimer's disease (*1*, *49*, *50*), which might be predicted to have effects on the NF-κB pathway and, consequently, AICD activity.

The detailed mechanism by which activation of the NF-κB pathway inhibits AICD activity remains to be determined. Possibilities include (i) direct IKK phosphorylation of AICD, (ii) sequestration by NF-κB of a transcriptional coactivator necessary for AICD activity, or (iii) NF-κB-dependent transcription of a gene whose product then inhibits the activity of AICD, among others. With regard to the second of these possibilities, it has recently been shown that both IL-1β and the AICD−Fe65−Tip60 complex can independently activate transcription from the p50 homodimer-binding NF-κB site of the KAI1 gene promoter by assembling distinct promoter complexes (*31*). In the former case, the complex minimally contains Tip60 and Bcl3; in the latter, it minimally contains Bcl3, AICD, Fe65, and Tip60. Both of these complexes displace an N−CoR corepressor complex from this promoter (*31*). We have thus far not been able detect a change in the Fe65−Tip60 interaction (Figure 5B,C). A possibility that cannot be ruled out by these experiments is that IL-1β directs Tip60 (or a yet to be identified Tip60 associated coactivator) to NF-κB-driven promoters, thereby decreasing the cellular pool of Tip60 that might otherwise be available to bind the AICD−Fe65 complex.

With regard to the last of these possibilities, it is relevant to note that NF-κB inhibits the JNK pathway through the transcription of specific genes that inhibit activation of the latter pathway (*51*−*53*). In the case of the AICD pathway, such genes, if they were to exist, might themselves be the targets for pharmaceutical intervention in the treatment of Alzheimer's disease.

ACKNOWLEDGMENT

We are grateful to Drs. Virginia Lee, Warner Greene, Carlos Paya, Roger Davis, Richard Treisman, and Olivia Pereira-Smith for gifts of plasmids. We thank Dr. Virginia Lee for providing the N2a cell line. We also thank Dr. Lee, Dr. Jianhe Huang, and Zheng Tu for critical readings of the manuscript.

REFERENCES

1. Hardy, J., and Selkoe, D. J. (2002) *Science 297*, 353−356.
2. Sisodia, S. S., and St. George-Hyslop, P. H. (2002) *Nat. Rev. Neurosci. 3*, 281−290.
3. Walter, J., Kaether, C., Steiner, H., and Haass, C. (2001) *Curr. Opin. Neurobiol. 11*, 585−590.
4. Fiore, F., Zambrano, N., Minopoli, G., Donini, V., Duilio, A., and Russo, T. (1995) *J. Biol. Chem. 270*, 30853−30856.
5. McLoughlin, D. M., and Miller, C. C. (1996) *FEBS Lett. 397*, 197−200.
6. Guenette, S. Y., Chen, J., Jondro, P. D., and Tanzi, R. E. (1996) *Proc. Natl. Acad. Sci. U.S.A. 93*, 10832−10837.
7. Borg, J. P., Ooi, J., Levy, E., and Margolis, B. (1996) *Mol. Cell. Biol. 16*, 6229−6241.
8. Zambrano, N., Buxbaum, J. D., Minopoli, G., Fiore, F., De Candia, P., De Renzis, S., Faraonio, R., Sabo, S., Cheetham, J., Sudol, M., and Russo, T. (1997) *J. Biol. Chem. 272*, 6399−6405.
9. Cao, X., and Sudhof, T. C. (2001) *Science 293*, 115−120.
10. Scheinfeld, M. H., Ghersi, E., Laky, K., Fowlkes, B. J., and D'Adamio, L. (2002) *J. Biol. Chem. 277*, 44195−44201.
11. Selkoe, D. J. (2001) *Proc. Natl. Acad. Sci. U.S.A. 98*, 11039−11041.
12. Panin, V. M., and Irvine, K. D. (1998) *Semin. Cell Dev. Biol. 9*, 609−617.
13. Artavanis-Tsakonas, S., Rand, M. D., and Lake, R. J. (1999) *Science 284*, 770−776.
14. Kadesch, T. (2000) *Exp. Cell Res. 260*, 1−8.
15. Pearson, G., Robinson, F., Beers Gibson, T., Xu, B. E., Karandikar, M., Berman, K., and Cobb, M. H. (2001) *Endocr. Rev. 22*, 153−183.

16. Weston, C. R., and Davis, R. J. (2002) *Curr. Opin. Genet. Dev. 12*, 14−21.
17. Ghosh, S., and Karin, M. (2002) *Cell 109* (Suppl.), S81−S96.
18. Widmann, C., Gibson, S., Jarpe, M. B., and Johnson, G. L. (1999) *Physiol. Rev. 79*, 143−180.
19. Silverman, N., and Maniatis, T. (2001) *Genes Dev. 15*, 2321−2342.
20. Senftleben, U., Cao, Y., Xiao, G., Greten, F. R., Krahn, G., Bonizzi, G., Chen, Y., Hu, Y., Fong, A., Sun, S. C., and Karin, M. (2001) *Science 293*, 1495−1499.
21. Cao, Y., Bonizzi, G., Seagroves, T. N., Greten, F. R., Johnson, R., Schmidt, E. V., and Karin, M. (2001) *Cell 107*, 763−775.
22. Malinin, N. L., Boldin, M. P., Kovalenko, A. V., and Wallach, D. (1997) *Nature 385*, 540−544.
23. Yin, L., Wu, L., Wesche, H., Arthur, C. D., White, J. M., Goeddel, D. V., and Schreiber, R. D. (2001) *Science 291*, 2162−2165.
24. Yang, J., Lin, Y., Guo, Z., Cheng, J., Huang, J., Deng, L., Liao, W., Chen, Z., Liu, Z., and Su, B. (2001) *Nat. Immunol. 2*, 620−624.
25. Zhao, Q., and Lee, F. S. (1999) *J. Biol. Chem. 274*, 8355−8358.
26. Tu, Z., Kelley, V. R., Collins, T., and Lee, F. S. (2001) *J. Immunol. 166*, 6839−6846.
27. Lin, X., Mu, Y., Cunningham, E. T., Jr., Marcu, K. B., Geleziunas, R., and Greene, W. C. (1998) *Mol. Cell. Biol. 18*, 5899−5907.
28. Brown, K., Gerstberger, S., Carlson, L., Franzoso, G., and Siebenlist, U. (1995) *Science 267*, 1485−1488.
29. Brockman, J. A., Scherer, D. C., McKinsey, T. A., Hall, S. M., Qi, X., Lee, W. Y., and Ballard, D. W. (1995) *Mol. Cell. Biol. 15*, 2809−2818.
30. Baeuerle, P. A., and Henkel, T. (1994) *Annu. Rev. Immunol. 12*, 141−179.
31. Baek, S. H., Ohgi, K. A., Rose, D. W., Koo, E. H., Glass, C. K., and Rosenfeld, M. G. (2002) *Cell 110*, 55−67.
32. O'Neill, L. A., and Greene, C. (1998) *J. Leukocyte Biol. 63*, 650−657.
33. Gao, Y., and Pimplikar, S. W. (2001) *Proc. Natl. Acad. Sci. U.S.A. 98*, 14979−14984.
34. Biederer, T., Cao, X., Sudhof, T. C., and Liu, X. (2002) *J. Neurosci. 22*, 7340−7351.
35. McGeer, P. L., and McGeer, E. G. (2001) *Neurobiol. Aging 22*, 799−809.
36. Mrak, R. E., and Griffin, W. S. (2001) *Neurobiol. Aging 22*, 903−908.
37. Perry, R. T., Collins, J. S., Wiener, H., Acton, R., and Go, R. C. (2001) *Neurobiol. Aging 22*, 873−883.
38. Boissiere, F., Hunot, S., Faucheux, B., Duyckaerts, C., Hauw, J. J., Agid, Y., and Hirsch, E. C. (1997) *Neuroreport 8*, 2849−2852.
39. Kaltschmidt, B., Uherek, M., Volk, B., Baeuerle, P. A., and Kaltschmidt, C. (1997) *Proc. Natl. Acad. Sci. U.S.A. 94*, 2642−2647.
40. O'Neill, L. A., and Kaltschmidt, C. (1997) *Trends Neurosci. 20*, 252−258.
41. Cotman, C. W. (1998) *Neurobiol. Aging 19*, S29−S32.
42. Karin, M., and Lin, A. (2002) *Nat. Immunol. 3*, 221−227.
43. Kaltschmidt, B., Uherek, M., Wellmann, H., Volk, B., and Kaltschmidt, C. (1999) *Proc. Natl. Acad. Sci. U.S.A. 96*, 9409−9414.
44. Wang, C. Y., Mayo, M. W., Korneluk, R. G., Goeddel, D. V., and Baldwin, A. S., Jr. (1998) *Science 281*, 1680−1683.
45. Chu, Z. L., McKinsey, T. A., Liu, L., Gentry, J. J., Malim, M. H., and Ballard, D. W. (1997) *Proc. Natl. Acad. Sci. U.S.A. 94*, 10057−10062.
46. Tamatani, M., Che, Y. H., Matsuzaki, H., Ogawa, S., Okado, H., Miyake, S., Mizuno, T., and Tohyama, M. (1999) *J. Biol. Chem. 274*, 8531−8538.
47. Lee, H. H., Dadgostar, H., Cheng, Q., Shu, J., and Cheng, G. (1999) *Proc. Natl. Acad. Sci. U.S.A. 96*, 9136−9141.
48. Kinoshita, A., Whelan, C. M., Berezovska, O., and Hyman, B. T. (2002) *J. Biol. Chem. 277*, 28530−28536.
49. Hoozemans, J. J., Rozemuller, A. J., Veerhuis, R., and Eikelenboom, P. (2001) *BioDrugs 15*, 325−337.
50. Yamamoto, Y., and Gaynor, R. B. (2001) *J. Clin. Invest. 107*, 135−142.
51. Kyriakis, J. M. (2001) *Nature 414*, 265−266.
52. De Smaele, E., Zazzeroni, F., Papa, S., Nguyen, D. U., Jin, R., Jones, J., Cong, R., and Franzoso, G. (2001) *Nature 414*, 308−313.
53. Tang, G., Minemoto, Y., Dibling, B., Purcell, N. H., Li, Z., Karin, M., and Lin, A. (2001) *Nature 414*, 313−317.

BI027117F